International Journal of Modern Physics E
Vol. 17, No. 5 (2008) 930–939

World Scientific
www.worldscientific.com

A COMPUTATIONAL MODEL FOR LESION DYNAMICS IN MULTIPLE SCLEROSIS OF THE BRAIN

T. R. KRISHNA MOHAN
Department of Pharmaceutical Sciences, State University of New York at Buffalo
Buffalo, NY 14260-1200, USA
kmohan@buffalo.edu

SURAJIT SEN
Department of Physics, State University of New York at Buffalo
Buffalo, NY 14260-1500, USA
sen@dynamics.physics.buffalo.edu

MURALI RAMANATHAN
Department of Pharmaceutical Sciences, State University of New York at Buffalo
Buffalo, NY 14260-1200, USA
murali@buffalo.edu

1. Abstract

Multiple sclerosis (MS) is a chronic disabling disease of the central nervous system (CNS) that is characterized by lesions with inflammatory cells, axons with the insulating myelin sheath damaged, and axonal loss. The causes of MS are not known and there is as yet no cure. The purpose of this research was to evaluate a physically motivated network model for lesion formation in the brain. The parsimonious network model contained two elements: (i) a spatially spreading pathological process causing cell damage and death leading to neuro-degeneration and, (ii) generation of alarm signals by the damaged cells that lead to activation of programmed death of cells surrounding the lesions in an attempt to contain the spatial spread of the pathologic process. Simulation results with a range of network geometries indicated that the model was capable of describing lesion progression and arrest. The modeling results also demonstrated dynamical complexity with sensitivity to initial conditions.

2. Introduction

MS is a chronic disease of the central nervous system (CNS) that affects about one million people worldwide and causes physical and cognitive disability. There are three types of MS: relapsing-remitting, secondary progressive and primary progressive, that differ in the dynamical patterns of disease progression. There are as

yet no known cures for MS. Patients with relapsing MS are currently treated with drugs that exert immunomodulatory effects and slow the progression of the disease; there are no effective treatment options for the progressive forms of MS.[1]

MS is postulated to be a cell-mediated autoimmune disease directed against myelin components of the CNS; myelin is an electrically insulating phospholipid layer that surrounds the axons of many neurons. The disease is characterized by both inflammatory immune responses and neuro-degeneration. The prevailing hypothesis on MS pathogenesis is that auto-reactive T lymphocytes, a cell type in the immune system, orchestrate a complex cascade of events that cause blood brain barrier disruption and invasion of immunologically aggressive cells into the CNS. However, the exact causes of MS still remain unknown.[2]

The histopathological hallmark of MS are the lesions, and delineating the tissue injury mechanisms involved in lesion formation is important for identifying the cause(s) of the MS and for developing targeted therapeutic strategies. The prevailing consensus on the causes for the lesions is that of a T-cell dependent, macrophage-mediated, autoimmune attack against constituents of the normal myelin sheath and the oligodendrocytes, which are the myelin generating cells of the CNS. The long-term goals of our research are to develop disease models that can be used to evaluate therapeutic strategies for this disease and, in this report, we specifically focus on evaluating a network model for MS lesion dynamics. To our knowledge, network approaches have not been studied extensively for disease modeling in MS.

2.1. *Previous work*

MS is an auto-immune disease and the simplistic models for auto-immunity are premised on the occurrence of defects in the immune system that cause it to turn against the host tissue. A defect-free immune system, in this world view, purportedly only attacks pathogens, the external agents that cause illness or disease.[3] However, an alternative viewpoint has been advocated where auto-immunity is seen as the usual immune response, but directed against those components of the body which, in normal conditions, are inaccessible to the immune system.[4–8] In the *danger model*, developed by Matzinger and collaborators, it is posited that stressed and injured tissues can mediate immune responses through the generation of appropriate "danger" signals; they stressed the importance of "danger" signals for activation of immune system as opposed to the need for recognizing external pathogenic cell types from host tissue.[6] The concept of *comprehensive immunity*, developed by Nevo et al. complements this perspective;[7] experimental studies supporting this idea were also carried out.[8] These refined immuno-biological models are more versatile and provides explanations for a wider range of experimental observations. A mathematical model developed by Smirnova and Stepanova in two variables, representing concentrations of tissue cells and immune cells (lymphocytes) respectively, without any external pathogens, reproduced the main dynamical patterns of auto-immune diseases.[5] A spatio-temporal mathematical model, in 1D space, illustrating

the structure of comprehensive immunity, was also developed be Nevo *et al.*[9] Our network model is inspired by these ideas.

The key elements of our model consist of a pathological process that causes cellular damage and programmed cell death initiated through an inter-cellular signaling component. The programmed cell death occurs in the periphery of the pathologically affected region and deprives the pathological process of healthy tissue which is necessary for its propagation in space and time. In this, it resembles the action of firemen who burn peripheral vegetation to contain forest fires. Inter-cellular signaling is a key feature of the model that allow pathologically damaged cells to propagate alarm signals and initiate programmed cell death in the boundary of the affected region. The exact causes of the pathologically induced cellular damage are not represented, but only its rate of migration through the network. Also, the mechanics of the cellular damage through programmed cell death is not modeled, but only the extent and location of it. The two processes are cast on a two dimensional network geometry to construct a description of the spatio-temporal evolution of damaged areas (identifiable as lesions) in the network. The model simulations demonstrate that it is capable of generating a large variety of lesion growth and arrest scenarios.

3. Model

An undirected, fixed radius random graph $G(n, r)$, with n nodes (vertices) and radius of connectivity, r, is constructed to represent the CNS in this 2D network model; fixed radius implies that nodes are connected only if they are within a distance of r. Biologically, the nodes of the graph can be viewed as representing cell bodies or functional units and the edges (bonds) of the graph can be viewed as axons or the interconnections between functional units.

We denote by d_i the degree of the ith node, i.e. the number of edges attached to it. Each edge was assigned a weight, $w(j)$ $(j = 1, \ldots, d_i)$, an integer number ranging from $0 \cdots w_{max}$, indicating its health. Edges with weight w_{max} are fully functional or healthy units, and those with weight zero, are dead. At the beginning of simulation, all edges of the network are assigned the maximum weight, w_{max}.

At time $t = 0$, the pathological process was initiated in a localized region of radial distance $ROI_{t=0}$ around the center. In the pathological process, the edges are damaged by lowering their weight by a single unit. However, in the programmed cell death process, edge weights are directly reduced to zero. In the regeneration process, edge weights are raised by a unit.

The pathological and regeneration processes are driven by probabilistic events wherein each edge in the affected region, in each time unit, has a certain probability $\mathbf{p}_d$ $(\mathbf{p}_r)$ of getting damaged (regenerated). In the general case, $\mathbf{p}_d$ $(\mathbf{p}_r)$ is a column vector of length w_{max} containing the transition probabilities from one state of health to another. Probability of programmed cell death, p_p, is independent of the health status of the edge.

The functional or health status of the ith node is the sum over its edge weights, $s_i(t) = \sum_{j=1}^{d_i} w(j)$. The maximum possible value of s_i is denoted by S_i and refers to its fully functional/healthy state. The value of S_i is realized when each edge of the node has weight w_{max}.

A node damaged by the pathological process generates an alarm signal when the ratio of its health status to the fully healthy state, $s_i(t)/S_i$, falls below a threshold, τ_{al}. The capacity of a node to monitor its own state of health and send out appropriate signals is what is indicated by τ_{al}. Such features are known to exist as in, for example, the generation of different antigens presented by cells dying natural or unnatural deaths. Programmed cell death is initiated at all the nodes where the propagated signals reach a threshold τ_{pr}. The system's capacity to detect the alarm signals and respond to them appropriately is what is modeled by τ_{pr}. The programmed cell death engulfs a semi-circular region, oriented towards the spreading direction of pathological damage, of size proportional to C_{bf}. Parameter C_{bf} is independent of the location of the node, and is considered here to be a characteristic capacity of the system. No signal is generated at any of the nodes in the programmed death region unlike the alarm signal generated in the pathologic process. Further, all remaining alarm signals in this region are reset to zero.

When signals are propagated, the signals received at the ith node are summed and they will be propagated further when the summed signal strength reaches S_i. The amplitude of the signal propagated along an edge is equal to its edge weight.

The spread of the pathologic process was driven by the success rate in causing cellular damage. The fraction of edges damaged in a particular time step, among the total number of edges in the affected area, was computed as the rate of damage due to the pathologic process, $R_I(t)$. The radius of the region affected by the pathologic process increased or decreased according to the formula, $(R_I(t) - R_0) \times ROI_{t=0}$, where $R_0 = 0.05$ was a threshold for viable growth. In a similar fashion, the region of programmed cell death was computed as $C_{bf} \times ROI_{t=0}$. Thus, $ROI_{t=0}$ sets a spatial scale in the problem.

4. Results

In this initial report, we only present the results for a two-state model with $w_{max} = 1$, i.e., there are no intermediate states of health and the edges are either alive or dead. Additionally, the regeneration probability was set to zero in order to focus exclusively on the effects of the pathological and programmed cell death processes on lesion structure and dynamics. We have set $n = 400$ and chosen a uniform random distribution of points in the unit square $[0, 1] \times [0, 1]$. The radius of connectivity was set to $r = 0.2$. An average degree strength of $d_{avg} = 13.82$ (standard deviation= 2.3) is obtained in this configuration with a minimum of 5 and a maximum of 25 edges to any node. There are a total of 2766 edges and the degree distribution is poissonian. The pathological process was initiated at $t = 0$ in a region of $ROI_{t=0} = 0.1$ around the center at (0.5, 0.5).

A probability of pathologic damage $p_d = 0.33$ was used, i.e. on average, one-third of the healthy edges in the affected region get damaged per unit time. For the programmed cell death, the probability p_p was set to 0.8. We varied τ_{pr} and C_{bf} to identify the conditions under which the pathological process could be controlled by the programmed cell death initiated at the boundary of the pathologically affected region. Larger values of τ_{pr} indicate reduced sensitivity to the alarm signals, whereas a larger value of C_{bf} indicates that a larger area near the alerted node is affected during the programmed cell death. We expected that a combination of increased sensitivity to the alarm signal (low τ_{pr}) and larger area over which programmed cell death is initiated should favor lesion arrest. However, it is also important to minimize total damage to the system.

The results are shown in Figs. 1–4. In these figures, the top left panel gives the number of edges damaged at time t via the pathologic and programmed cell death processes. The top right panel gives the cumulative number of edges damaged since $t = 0$ and the contributions of pathologic and programmed cell death processes to the cumulative damage. The bottom left panel gives the rate of pathological damage at time t, $R_I(t)$ and the bottom right panel gives a snapshot of the lesion in the network at the end of the simulation.

In Fig. 1, we have the system capacity for initiating programmed cell death, i.e. the area over which the programmed cell death is triggered near an alerted node, set low at $C_{bf} = 0.5$. The parameter τ_{pr} is set to 0.8, which indicates a low sensitivity to the alarm signals, i.e. programmed cell death is only activated upon the alarm signal strength reaching a threshold of 0.8. We find that the pathological damage process is not controlled, though it has been brought down to lower levels (Fig. 1(c)). The number of pathologically damaged edges keeps growing with time (Figs. 1(a) and (b)) because, although the rate of pathological damage is lower than at the beginning, the affected area is larger and almost equal to the whole network by $t = 20$ (Fig. 1(d)). The number of edges damaged by the programmed cell death is very few and insufficient to control the pathologic damage (Fig. 1(a)); even the cumulative number of edges damaged by programmed cell death is hardly significant (Fig. 1(b)). We note that almost the entire damage is, therefore, caused by the pathological process. It is then also clear that, in the absence of the programmed cell death process (not shown here), the damage due to the pathological process is even higher.

In Fig. 2, we have maintained the capacity of the programmed cell death process at $C_{bf} = 0.5$ and increased the sensitivity to alarm signals by lowering the threshold τ_{pr} to 0.4. The pathologic process gets arrested now, as seen from the bottom left panel (Fig. 2(c)), at around the time, $t = 20$; we recall that, in the same time period, the whole network was damaged in the earlier case. The cumulative number of damaged edges is approximately 1800 (Fig. 2(b)), which is significant, being (2/3)rd of the total number of edges (= 2766). Indeed, we see, from Fig. 2(d), that the damage has almost reached the boundaries (boundary effects will be taken care of in a future work), but is still lesser, even visually, than in Fig. 1(d). We note

that the increased sensitivity to the alarm signals has brought up, to significant levels, the number of damaged edges due to programmed cell death, as compared to the earlier case in Fig. 1.

Now, we set the capacity of programmed cell death process high at $C_{bf} = 0.8$, i.e. more area near an alerted node will be damaged when programmed cell death is initiated, and the results are given in Figs. 3–4. Sensitivity to the alarm signal is set low with a high threshold of $\tau_{pr} = 0.8$ in Fig. 3. We find that the pathologic process is controlled (Fig. 3(c)) at around the same time, $t = 20$, as in Fig. 2(c), but with reduced cumulative damage (Fig. 3(b)), compared to Fig. 2(b); only about (1/3)rd of the total edges are damaged compared to the (2/3)rd that was damaged

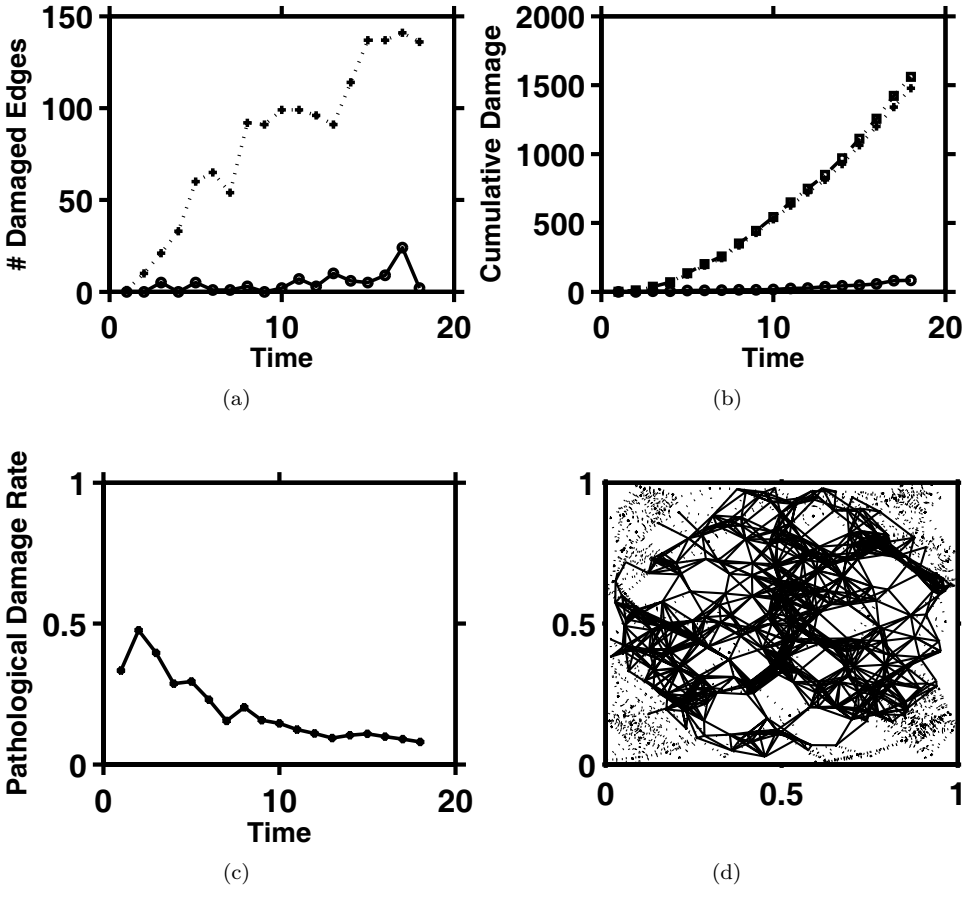

Fig. 1. In the top panels, '+' marks pathologic process and 'o' marks immune mediated programmed cell death process. The square symbol in top right panel marks sum total of damage due to both processes. In bottom right panel, dotted lines indicated healthy edges and the bold lines, damaged edges. Parameters: System capacity for programmed cell death, $C_{bf} = 0.5$; Sensitivity to alarm signals, $\tau_{pr} = 0.8$.

in the last case. We also see that the reduced cumulative damage is due to reduced damage from the pathologic process and the extent of cumulative damage from programmed cell death is approximately the same.

The sensitivity to the alarm signals has been raised in Fig. 4 by lowering the threshold τ_{pr} to 0.4, while maintaining the high capacity for programmed cell death, $C_{bf} = 0.8$. The lesion structure in Fig. 4(d) covers the least area among all the ones seen so far in Figs. 1–4. This fact is readily borne out by the cumulative damage shown in Fig. 4(b) which, again, is the least seen so far and significantly less than 1000; it is only around 750 damaged edges which is just about 27% of the total number of edges. Notice, however, that the time to control the pathologic process is not significantly different from Figs. 2–3; it still takes around $t = 20$ units. This may have to do with the spatial time scale set in the problem, given by $ROI_{t=0} = 0.1$; this is currently under investigation.

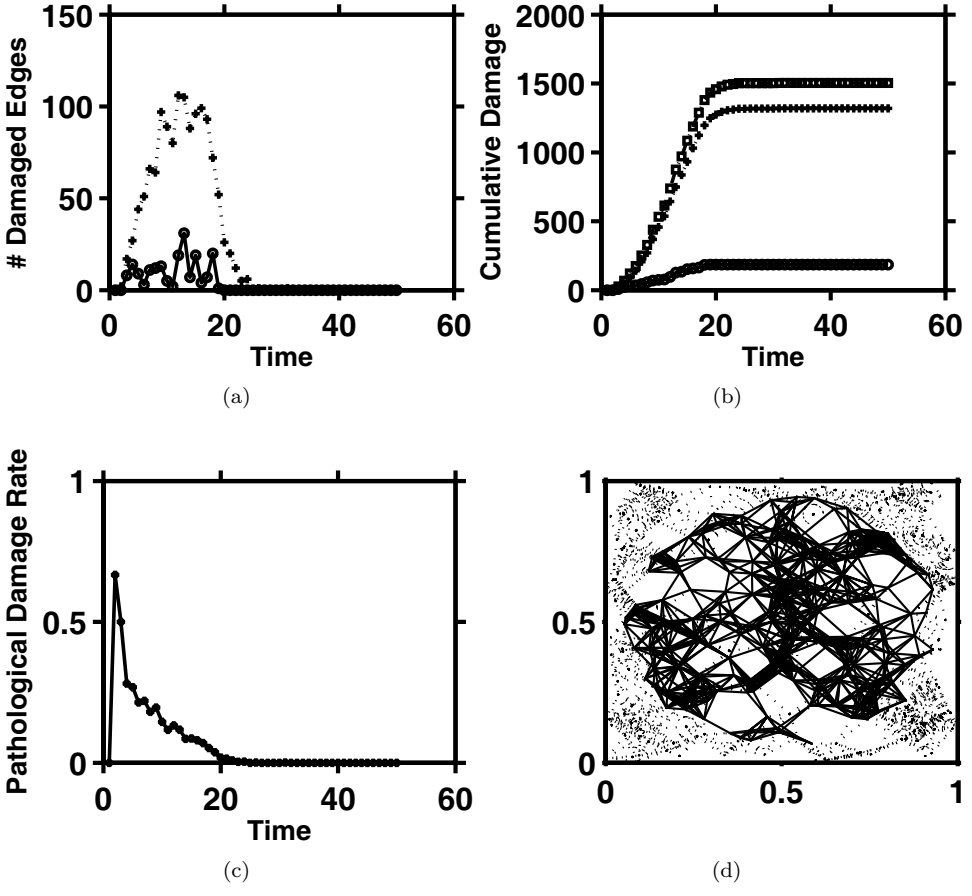

Fig. 2. Figure legends as in Fig. 1. Parameters: $C_{bf} = 0.5$; $\tau_{pr} = 0.4$.

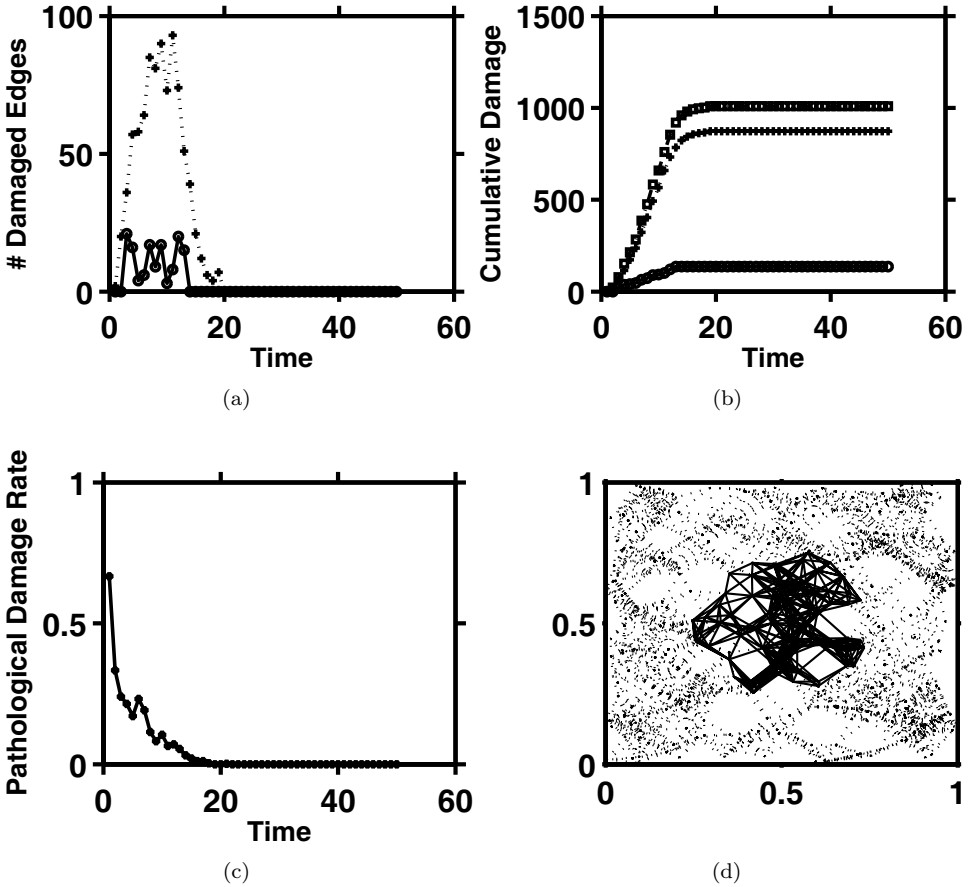

Fig. 3. Figure legends as in Fig. 1. Parameters: $C_{bf} = 0.8$; $\tau_{pr} = 0.8$.

We have also investigated regular lattices. Three types of 2D lattices, square, triangular and hexagonal lattices, each with $n = 400$ lattice points in the unit square $[0, 1] \times [0, 1]$, were studied. The lattice spacing in the x and y directions was 0.05 for square and triangular lattices; the y-spacing was changed to $\sqrt{3}/2 \times x$-spacing for the hexagonal lattice. Radius of connectivity was kept at $r = 0.2$ for all the three regular lattices. The total number of edges in these graphs with this configuration turns out to be 3721 for triangular lattice, 3812 for hexagonal lattice and 3996 for square lattice. The average degree strengths were 18.59, 18.98 and 19.83 for the triangular, hexagonal and square lattices respectively, with the degree distribution skewed towards the higher degree strengths. Both the total number of edges and the average degree strengths are significantly higher for these regular lattices. Our initial results indicate that the higher average degree strengths of regular lattices prevent early control of the pathologic process.[10]

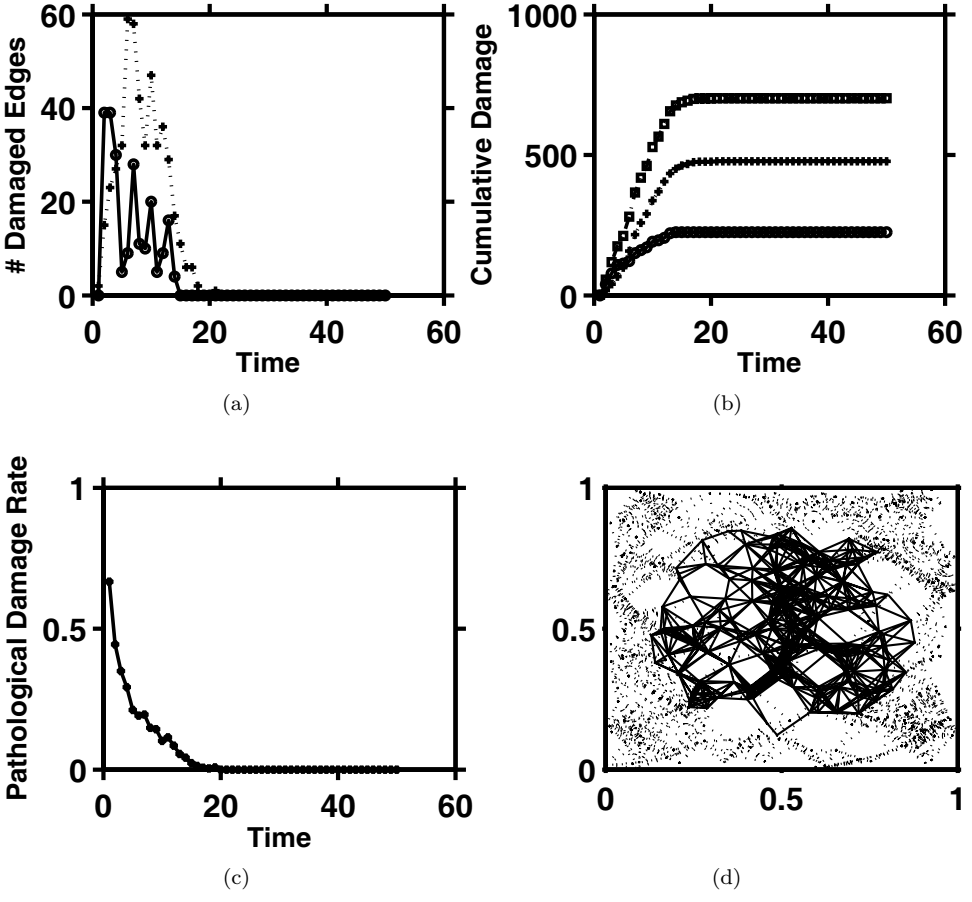

(a) (b) (c) (d)

Fig. 4. Figure legends as in Fig. 1. Parameters: $C_{bf} = 0.8$; $\tau_{pr} = 0.4$.

5. Conclusions

A physically motivated model was developed for the CNS and employed to study the process of lesion formation in MS. The model demonstrates that the spread of the pathologic process can be arrested by programmed cell death in the periphery of the lesions. This process is akin to removal of peripheral vegetation to control forest fires. The arrest of the lesion growth in the pathologic process depends crucially on the two parameters, τ_{pr} and C_{bf}. The parameter τ_{pr} controls the sensitivity of the system to signals generated by the pathologically damaged tissues. The parameter C_{bf}, a characteristic capacity of the system, sets the size of the region in which programmed cell death can be initiated. High sensitivity and larger capacity guarantees early arrest of degeneration with minimal damage, whereas low sensitivity and low capacity may even lead to failure in controlling the pathologic damage.

Acknowledgments

We acknowledge the support of the UB2020 Scholar's Fund. Dr. Murali Ramanathan also acknowledges funding from the University at Buffalo and Pfizer Inc.

References

1. O. Kantarci and D. Wingerchuk, *Curr. Opin. Neurol.* **19** (2006) 248; T. J. Murray, *Brit. Med. J.* **332** (2006) 525.
2. M. Sospedra and R. Martin, *Ann. Rev. Immunol.* **23** (2005) 683; V. H. Perry and D. C. Anthony, *Philos. T. Roy. Soc. B* **354** (1999) 1641.
3. F. M. Burnet and F. Fenner, *The Production of Antibodies* 2nd edn. (MacMillan, Melbourne, 1949); F. M. Burnet (ed.), *Immunology: Readings from Scientific American* (W. H. Freeman, San Francisco, 1976); E. Christ and A. I. Tauber, *Biol. Philos.* **15** (1999) 509.
4. G. J. V. Nossal, *Antibodies and Immunity* 2nd edn. (Basic Books, New York, 1978).
5. O. A. Smirnova and N. V. Stepanova, *Biofizika* **20** (1975) 1095.
6. P. Matzinger, *Ann. Rev. Immunol.* **12** (1994) 991; P. Matzinger, *Semin. Immunol.* **10** (1998) 399.
7. U. Nevo, J. Kipnis, I. Golding, I. Shaked, A. U. Neumann, S. Akselrod and M. Schwarz, *Trends Mol. Med.* **9** (2003) 88.
8. G. Moalem, R. Leibowitz-Amit, E. Yoles, F. Mor, I. R. Cohen and M. Schwartz, *Nat. Med.* **5** (1999) 49.
9. U. Nevo, I. Golding, A. U. Neumann, M. Schwarz and S. Akselrod, *J. Theo. Biol.* **227** (2004) 583.
10. T. R. Krishna Mohan, S. Sen and M. Ramanathan, unpublished results.